Author(s): Twum, Kwaku; Rautiainen, J. Mikko; Yu, Shilin Y.; Truong, Khai-nghi K. N.; Feder, Jordan; Rissanen, Kari; Puttreddy, Rakesh; Beyeh, Ngong Kodiah

Title: Host-Guest Interactions of Sodiumsulfonatomethyleneresorcinarene and Quaternary Ammonium Halides : An Experimental-Computational Analysis of the Guest Inclusion Properties

Year: 2020

Version: Accepted version (Final draft)

Please cite the original version:

Twum, K., Rautiainen, J. M., Yu, S. Y., Truong, K.-N. K. N., Feder, J., Rissanen, K., Puttreddy, R., & Beyeh, N. K. (2020). Host-Guest Interactions of Sodiumsulfonatomethyleneresorcinarene and Quaternary Ammonium Halides : An Experimental-Computational Analysis of the Guest Inclusion Properties. Crystal Growth and Design, 20(4), 2367-2376. https://doi.org/10.1021/acs.cgd.9b01540

CRYSTAL GROWTH & DESIGN

Article

Host-Guest Interactions of Sodiumsulfonatomethyleneresorcinarene and Quaternary Ammonium Halides: An Experimental-Computational Analysis of the Guest Inclusion Properties

Kwaku Twum, J. Mikko Rautiainen, Shilin Y. Yu, Khai-nghi K. N. Truong, Jordan Feder, Kari Rissanen, Rakesh Puttreddy, and Ngong Kodiah Beyeh

Cryst. Growth Des., **Just Accepted Manuscript** • DOI: 10.1021/acs.cgd.9b01540 • Publication Date (Web): 15 Jan 2020

Just Accepted

is published by the American Chemical Society. 1155 Sixteenth Street N.W., Washington, DC 20036

Host-Guest Interactions of Sodiumsulfonatomethyleneresorcinarene and Quaternary Ammonium Halides: An Experimental-Computational Analysis of the Guest Inclusion Properties†

Kwaku Twum,[a] J. Mikko Rautiainen,[b] Shilin Y. Yu,[b] Khai-Nghi K. N. Truong,[b] Jordan Feder,[a] Kari Rissanen,[b] Rakesh Puttreddy[b,c*] and Ngong Kodiah Beyeh[a*]

[a]*Oakland University, Department of Chemistry, 146 Library Drive, Rochester, Michigan, 48309-4479, USA*

[b]*Department of Chemistry, University of Jyvaskyla, Survontie 9 B, FI-40014 Jyväskylä, Finland*

[c]*Smart Photonic Materials, Faculty of Engineering and Natural Sciences, Tampere University, P. O. Box 541, FI-33101, Tampere, Finland*

ABSTRACT

The molecular recognition of nine quaternary alkyl- and aryl-ammonium halides (**Bn**) by two different receptors, C_{alkyl}-tetrasodiumsulfonatomethyleneresorcinarene (**An**), were studied in

solution using ^{1}H NMR spectroscopy. Substitution of methylenesulfonate groups at 2-positions of resorcinol units resulted in an increase of cavity depth by ~2.80 Å and a narrow cavity portal compared to C_{alkyl}-2-H-resorcinarenes. The effect of alkyl chain lengths on the *endo*-complexation, that is the ability to incorporate other than N-methyl chains inside the cavities, were investigated using ammonium cations of the type $^+NH_2(R_1)(R_2)$, (R_1 = Me, Et, Bu, R_2 = Bu, Ph, Bz). The C−H···π interactions between guests and hosts are the key driving forces for 14 out of 16 observed *endo*-complexes. In case of *N*-butyl-*N*-benzylammonium cation, the hydrogen bonding between -NH_2 and sulfonate oxygens and the larger size hamper the *N*-butyl and *N*-benzyl groups from entering the host cavity. Association constants derived from isothermal calorimetry titrations confirm 1:1 host-guest complexes highlighting guest affinity, based on size and orientation. X-Ray crystallographic analysis revealed two types of complexes *viz* sodium-containing co-crystals, [(**An**)$^{4-}$ · *m*(**Bn**)$^+$ · q**Na**$^+$], and sodium-free, [(**An**)$^{4-}$ · 4(**Bn**)$^+$]. Both types accommodate (**Bn**$^+$) guests in their cavities. The *N*-methylated heterocycle guests and host form capsule-like structures in which the two-halves were joined by O−Na coordination bonds and self-assembles in to 2-D polymeric sheets. From the crystal structures, different conformations of methylenesulfonate groups with respect to cavity arising due to tetrahedral geometry of methylene linker were observed. Density Functional Theory (DFT) computations were used to analyze the effects of *endo*-guests on host conformations and to estimate the relative strengths of host-guest interactions.

INTRODUCTION

Resorcinarenes as synthetic receptors are well-studied in the supramolecular host-guest (H-G) chemistry.[1–4] The development of aesthetic functionalization methods at the upper-rim such as alkylation/arylation of hydroxyl groups and the introduction of substituents at the C2-position

between two hydroxyl groups of resorcinol has notably made resorcinarene an excellent building block to produce extended structures for applications beyond the H-G studies.[5–7] The ability to modulate the properties of resorcinarenes by synthetic means has allowed the design of targeted molecules for self-assembly processes. This in turn has led to exotic materials with tunable chemical and physical properties.[8] Functionalized resorcinarenes have found use in nanoparticle synthesis,[9–12] optical[13,14] and chemosensors,[15] gels,[16] and separation applications.[17] In addition to the various potential applications of resorcinarenes, their use in rigorous quantitative H-G studies to extrapolate structure-property relationships and gain insights into fundamental principles e.g. guest binding affinities, size and shape, and conformational flexibility has always received wide attention in supramolecular chemistry research.[1] Unravelling such fundamental knowledge could help to build complex molecular systems using the bottom-up approach. The bottom-up approach in supramolecular chemistry has already created access for chemists to perform catalysis and organic reactions inside self-assembled hexamer and capsular structures [18–21] and has the potential for much more.

The major structural feature of resorcinarenes is the electron-rich cavity, formed by the circular intramolecular O···H–O hydrogen bonding interactions between adjacent resorcinol units that can bind neutral and cationic guests through C−H···π, cation···π, and/or cooperative H-bond interactions.[22] In case of guest shape and size mismatch, the host's cavity stabilizes either by self-inclusion[23–25] or solvent encapsulation.[26,27] *Exo*-guest complex formation arises often via competitive H-bond interactions resulting in co-crystal complexes.[23,28,29] The situation becomes even more complex when the H-G systems are in equilibrium with metal ions or highly H-bond competitive anions and the hosts are prevented from forming self-inclusion complexes. Sodiumsulfonatomethyleneresorcinarene is an example of a host that can interact with guests via

multiple functionalities (Figure 1). Sulfonate substitution makes the resorcinarenes behave as amphiphiles. This amphiphilic behavior of tetrasulfonate derivatives (SR) has created new avenues for harnessing resorcinarenes in biological applications.[30,31] The representative examples of SRs studied in the literature include, methylenesulfonate groups appended at the upper-rim C2-positions (Type-1),[30–41] sulfonate and phenolic oxygens linked by methylene chains (Type-2),[42] and alkylated sulfonate derivatives at the lower-rim (Type-3).[43–45] The nature of their binding to neutral, singly and doubly charged aliphatic/N-heterocycle cationic guests has been studied in solution to understand the sulfonate groups intricate role in H-G systems. For example, Liu *et al*. have shown that the H-G complexation between viologen type cationic guests and Type-2 receptor in water results from charge transfer interaction between electron-rich host and electron-deficient guest aromatic rings.[42] Additionally, the upper-rim longer alkyl chain sulfonates provide an elongated cavity to improve the binding affinity for rod-shaped guests such as *N*,*N*-dimethyl-4,4-bipyridinium ions. In another report by Aoyama *et al*., the recognition of sugars using Type-3 receptors in water resulted in very low binding constants due to the aggregation of lower-rim longer alkylsulfonate chains and competitive H-bonding interactions.[43] These findings demonstrate that the factors affecting the guest inclusion complexes depend on the inherent location of the sulfonate groups, and therefore, clearly understanding such principles governing the molecular recognition process is a valuable asset to H-G chemistry based applications.[35]

In this context, Type-1 receptors have been subjected to less systematic testing in H-G studies using cationic guests. Several of Type-1 host's intriguing properties and possibilities of their unique *endo*-cavity environments for molecular recognition in solid-state and solution have been underexplored. For rational design of H-G systems exploiting Type-1 receptors it is crucial to understand their limitations particularly in terms of spatial constraints of their cavities and nature

of their H-G interactions. In the present two-component approach, $\mathbf{An \cdot B_n}$ we use a combination of ^{1}H NMR spectroscopy, isothermal titration calorimetry, X-ray crystallography and computational studies, to investigate the nature of H-G chemistry between sodiumsulfonatomethyleneresorcinarene (**An**, **n** = **1**,**2**) and a set of nine ammonium guests (**Bn**, **n** = **1** - **9**) shown in Figure 1. Our motivation for studying the Type-1 receptors stem from the following: (i) the four sulfonate groups encompassing the upper-rim offer a deeper cavity compared to classic C_{ethyl}-2-H-resorcinarene, and these substituents should act as a lid rendering a narrow portal thus improving the guest selectivity, (ii) the guests can be stabilized by both C−H···π and C−H···OSO_2 interactions from *endo*-cavity π-systems and sulfonate groups, respectively, (iii) mixing host (**An**) and guest (**Bn**) components leads to desalination (meaning removal of sodium chloride or sodium iodide) and the formation of H-G complexes of the type $(\mathbf{An})^- \cdot (\mathbf{Bn})^+$, despite the strong electrostatic attractive interaction between sulfonate O-atom and sodium to form coordination complexes, and competitive hydrogen bond interactions between chloride ion and the ammonium cations' H-atoms, (iv) the type of H-G interactions favored in *endo*-guest complexes can be potentially tuned by changing the H-G size match and ammonium cation functional groups. We investigate the preferred type of H-G interactions by using a series of ammonium cations $^+NH_2(R_1)(R_2)$ (R_1 = -methyl, -ethyl; R_2 = -ethyl, -butyl, -aryl) to determine whether the *endo*-guest complexation occurs rather by more acidic *N*-methyl, *N*-ethyl or through longer *N*-alkyl/*N*-aryl chains. The $^+N(CH_3)_4$ is used as reference species as it is expected to have the best size match fitting inside the cavity and strong binding due to acidic C−H protons that can take part in C−H···π interactions. Furthermore, we investigate whether *N*-methylated heterocycles have the inclination to form *endo*-complexes via *N*-methyl or the aromatic π-system using guest **B8** and **B9**.

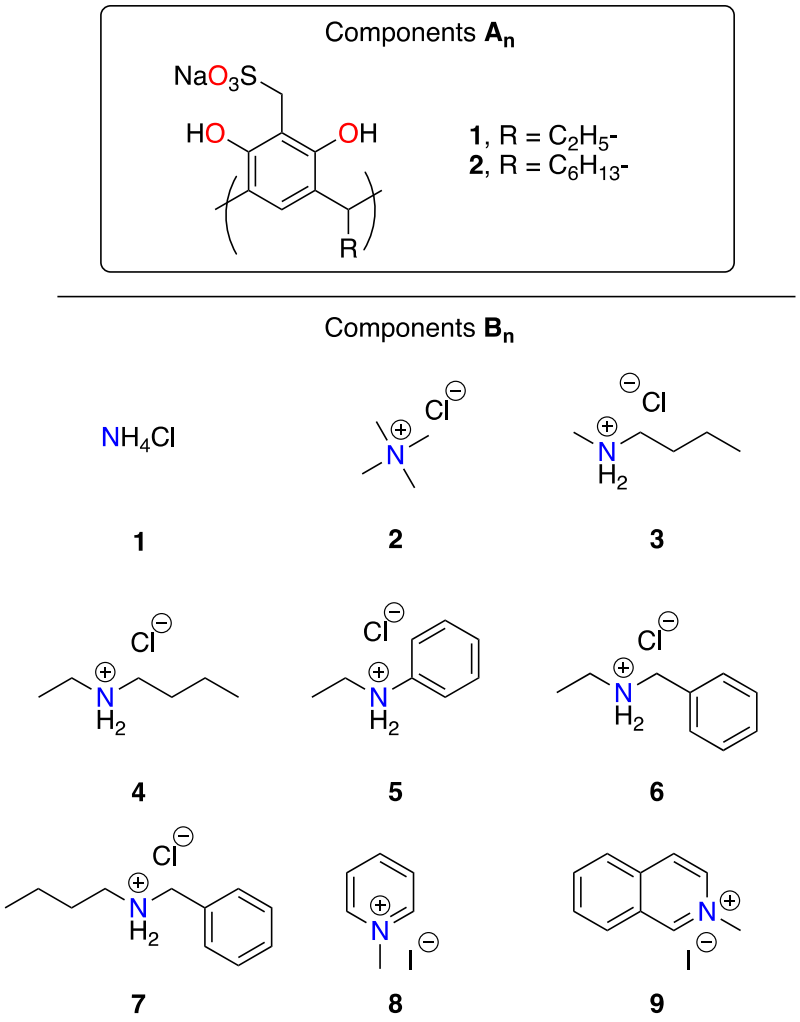

Figure 1. List of components, sodiumsulfonatomethyleneresorcinarene hosts **An** [**n** = **1**,**2**] (A), and quaternary ammonium halides **Bn** [**n** = **1**-**9**] (B).

RESULTS AND DISCUSSION

Solution studies

^{1}H NMR studies

The binding properties of the receptor **An** (**n** = **1**,**2**) towards the guests were probed in solution through ^{1}H NMR analyses. The major difference between **A1** and **A2** is the length of the lower-rim. The flexibility of resorcinarenes is reduced with increasing length of the lower rim chain.[1]

This limited flexibility of **A2** was observed through smaller shielding of the guest signals compared to **A1**. Additionally, changes in the aromatic (ArH) and methylene (-CH_2S-) signals of **A2** were much lower when compared to the same signals of **A1** in cases of identical guests, confirming the limited flexibility of **A2** (Figures S5-S11). The ^{1}H NMR data of **A2**, henceforth, is included in the supporting information while the main text discussion is based on H-G chemistry of **A1**.

In solution, the complexes are in rapid equilibrium with the free components, therefore, only one set of signals could be observed in the NMR spectra of the mixtures. Despite the dynamic system and fast exchange process, e*ndo*-cavity binding of the guests can be determined through monitoring the shielding effects of the guest signals. By following and comparing the degree of shielding, one could qualitatively determine which part of the $^+NH_2$(R1)(R2) guest (R1 or R2) is preferred and predominantly located in the cavity of the receptor. Strong increase in shielding of the guest **B2** protons was observed as would be expected considering the affinity of resorcinarenes towards quaternary ammonium ions. For the other guests, several parameters were investigated to understand the preferences of the host towards the guests **B1**-**B9**. First, we determined the maximum length of the alkyl group that could possibly be bound into the cavity of the receptor. For

this process, the H-G complexes between **A1** and **B3**-**B7** were investigated. Taking **A1** *vs* **B3** as an example, the *N*-methyl group of **B3** had the higher increase in shielding (1.62 ppm) when compared to the $–CH_3$ protons of the butyl group (0.14 ppm) clearly suggesting the *N*-methyl group sits deep into the cavity of the of **A1** (Figure 2B). By the same analyses, it was observed that the *N*-ethyl groups of **B4**, **B5** and **B6** are also preferred for the *endo*-complexation (Figures S2). Guest **B7** is a particularly interesting example, since it has a butyl group on one side and a benzyl group on the opposite side of the nitrogen. Following the ^1H NMR changes, it was observed that neither the terminal $–CH_3$ signals of the *N*-butyl group (0.24 ppm) nor the aromatic signals of the *N*-benzyl group (*a-proton*: 0.31 ppm) had the highest change in shielding. Instead, the methylene protons closest to the ammonium group ($N\text{-}CH_2\text{-}$) showed the highest increase in shielding (0.64 ppm, 0.66 ppm). This suggest that the receptor **A1** interacts with the carbons adjacent to the positively charged nitrogen of the guest **B7** as shown in Figure 2D.

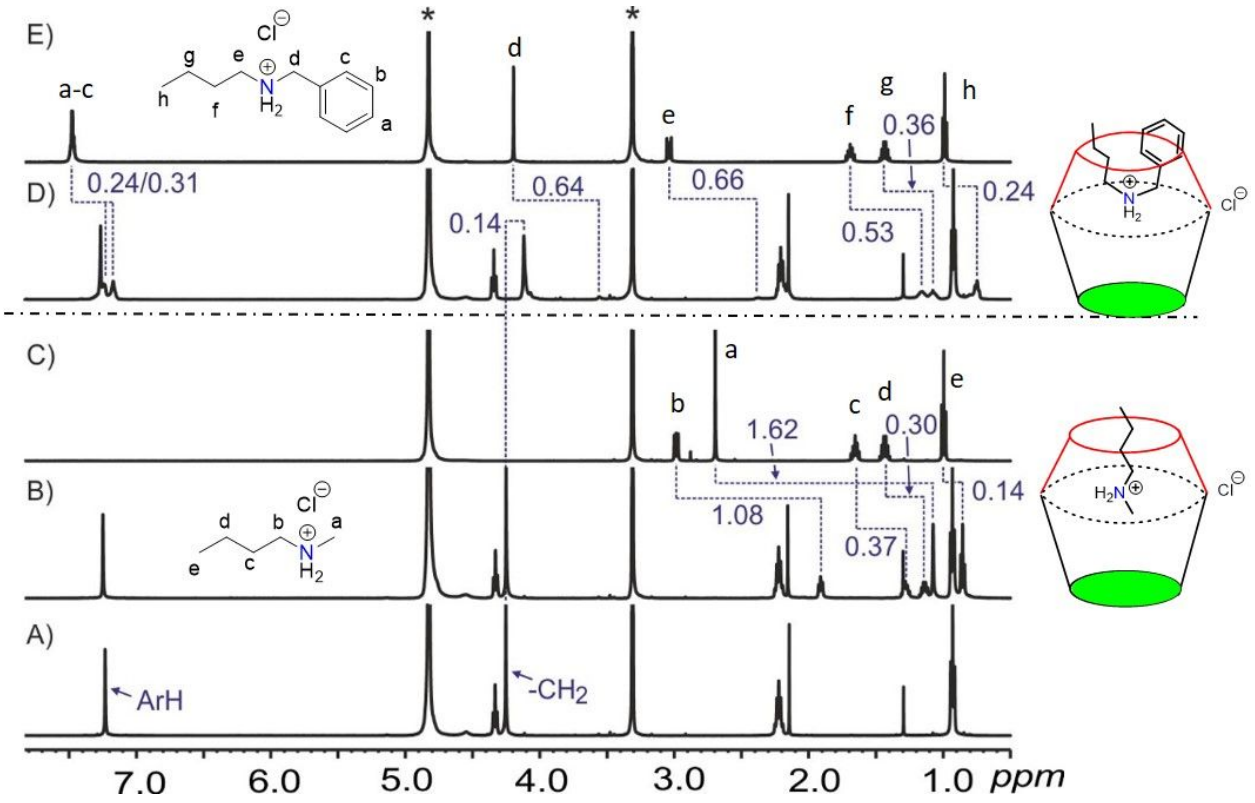

Figure 2. ^{1}H NMR spectra (CD_3OD, 303 K) of: (A) host **A1**, (C) guest **B3**, (E) guest **B7**, and the equimolar mixtures of (B) **A1** and **B3**, (D) **A1** and **B7**. Star represents the residual CD_3OD solvent. The dash lines give an indication of the signal changes in ppm.

Secondly, we compared whether interaction with *N*-methyl group or the aromatic ring of pyridinium ion in **B8** was preferred by the host. The changes in ^{1}H NMR of **B8** in host equilibrium show that the aromatic protons were located deeper into the cavity of **A1** than the *N*-methyl group (increase in shielding Ph_a: 1.63 ppm, *N*-CH_3: 0.95 ppm, Figure 3B). This is in contrasts with the *N*-ethyl group preference shown by the *endo*-complexation of **B5** or the preference toward shorter *N*-methyl or *N*-ethyl groups shown by the shallow cavity of host **A1** with the **B3**-**B7** guests. In case of **B8** the different behavior can be explained by the better size match and stronger π–π interactions between the electron-deficient pyridinium ion and the electron-rich cavity of the host **A1**. Next, in case of guest *N*-methylquinolinium iodide **B9**, the higher increase in shielding of ^{1}H NMR signals

of the *N*-methyl group show it to be located in the cavity of the receptor **A1** (increase in shielding Qu_g: 0.87 ppm, *N*-CH_3: 1.69 ppm, Figure S11). This preference could be explained by a better size match of *N*-methyl group than the quinoline moiety to the cavity of the host **A1**. Additionally, the larger π-system of **B9** is not as electron deficient as the aromatic ring in **B8**.

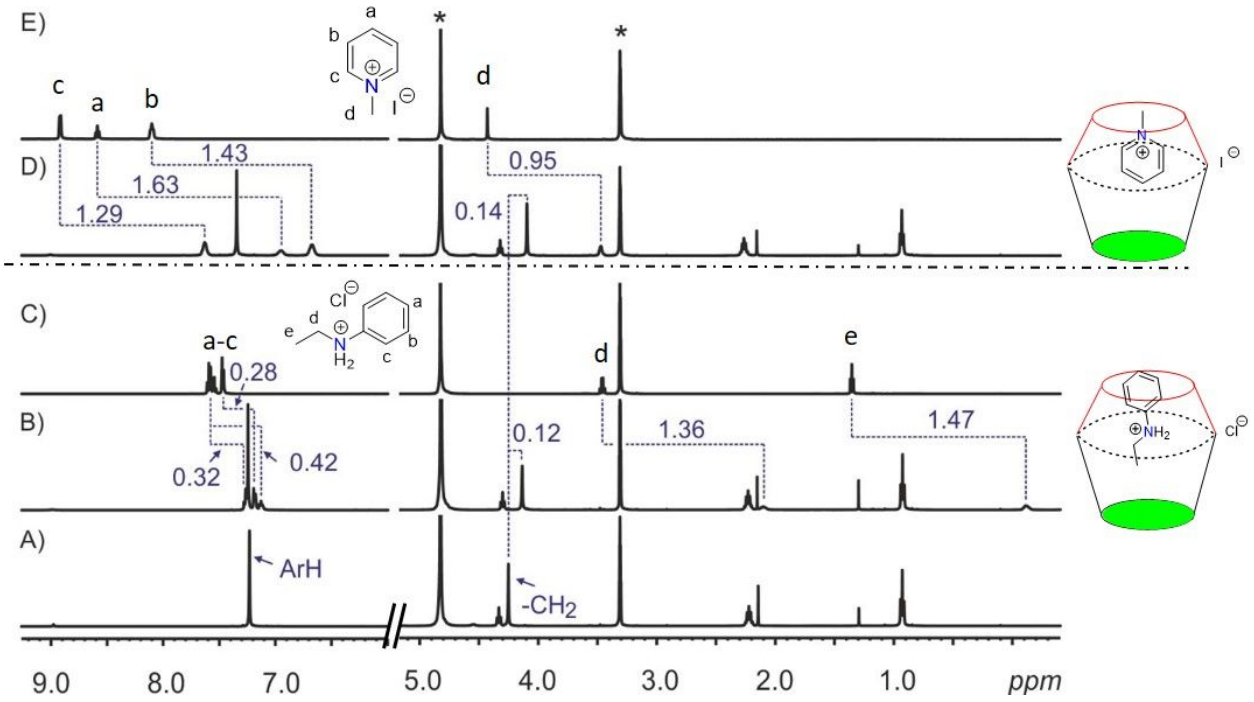

Figure 3. ^{1}H NMR spectra (CD_3OD, 303 K) of: (A) host **A1**, (C) guest **B5**, (E) guest **B8**, and the equimolar mixtures of (B) **A1** and **B5**, (D) **A1** and **B8**. Star represents the residual CD_3OD solvent. The dash lines give an indication of the signal changes in ppm.

Isothermal Titration Calorimetry (ITC)

The complexation of the guests **Bn** by the host **A1** were quantified through a series of ITC experiments in methanol (Figures S12-S14). The thermodynamic parameters of host-guest binding (K_a, ΔH, ΔS, and ΔG) between the host **A1** and the guests **Bn** were determined by fitting the ITC data to a one-site binding model (Table 1). Complex formation between any combination of the

host **A1** and the guests **Bn** is spontaneous ($\Delta G<0$) at the experimental temperature (303 K). The negative ΔH and positive $T\Delta S$ values indicate the complexation of the guests by **A1** are both enthalpy and entropy driven. Solvation of the species and the counter ion releases are factors that explain the entropy contribution. This has been previously observed for supramolecular binding interactions between poly(ammonium chlorides) and poly(sodium phosphates), and may be due to the particularly strong ion-pairs in the parent **A1** host.[46] The highest binding affinity among all the guests was observed with guest **B2** (K_a = 909 M^{-1}). This is logical since tetramethylammonium cation is known to be a good fit for resorcinarene cavity through C–H···π and cation–π interactions.[47–50] This value is much higher when compared with basic resorcinarenes in methanol (K_a ~ 100-200 M^{-1}).[27,49,51] The binding affinities for the rest of the guests (**B1**, **B4**, **B6** and **B9**) were similar which can be accounted for by the flexibility of the guests and size mismatch with the host cavity. The binding constants for **B6** and **B8** were slightly higher than **B1**, **B4**, **B7** and **B9**, and can be accounted for due to a better fit into the cavity of host **A1**. The weakest binding was observed with guest **B9**, which can be accounted for by its large size as compared to all the other guests.

Table 1. Thermodynamic binding parameters of formed complexes between the host **A1** and the guests **Bn** by ITC[a].

Complex	K_a M^{-1}	ΔH_1 kcal/mol	$T\Delta S_1$ kcal/mol	ΔG_1 kcal/mol
B1@A1	173.00±7.19	-2.58±0.15	10.40	-13.00
B2@A1	909.10±191.60	-13.80±0.18	3.37	-17.20

B3@A1	-[b]	-[b]	-[b]	-[b]
B4@A1	196.10±21.90	-8.77±0.07	4.54	-13.30
B5@A1	-[b]	-[b]	-[b]	-[b]
B6@A1	546.40±123.60	-9.28±0.07	6.63	-15.90
B7@A1	207.90±53.80	-6.62±0.07	6.84	-13.50
B8@A1	326.80±38.60	-7.12±0.07	7.49	-14.60
B9@A1	80.00±7.10	-12.50±0.07	-1.48	-11.02

[a]ITC was done in methanol at 303 K. [b]Data could not be obtained due to large errors.

X-Ray crystallography

Five H-G crystal structures were obtained by using **A1** (For more details, see Experimental section) while our attempts to crystallize H-G complexes of **A2** were unsuccessful. Complex **B1@A1**, obtained by mixing **A1**:**B1** in 1:10 molar ratio, is a co-crystal of the type $[(\mathbf{A1})^{4-} \cdot 4(\mathbf{B1})^{+}]$. The asymmetric unit contains two crystallographically independent $\mathbf{A1}^{4-}$ hosts. In one of the hosts, the four SO_3 groups encompassing the upper-rim of the host cavity are inwardly directed (4-*in*) to give a closed vase-like conformation. In the other host, three SO_3 groups are inward and the fourth is outwardly (3-*in*-1-*out*) directed as depicted in Figure 4. Due to the smaller guest size, the $\mathbf{B1}^{+}$ is *exo*-cavity bound via hydrogen-bonds to the sulfonate oxygens. The **A1** cavities are occupied by methanol molecules that are stabilized by C−H···π interactions with the shortest contact being *ca*. 2.847 Å in 4-*in* and 2.696 Å in 3-*in*-1-*out*. The term Gh is defined as the calculated distance from the centroid of lower-rim aromatic carbon atoms to the closest non-hydrogen atom of the guest. *Gh* values of methanol molecules are 2.90 Å and 2.88 Å for hosts, 4-*in* and 3-*in*-1-*out*, respectively. The **A1** in vase conformation can be defined as two truncated cones joined at the larger diameter side as shown in Figure 5. The dimensions, h_1 and h_2 are the heights of the bottom cone and the upper truncated cone extended by installing methylenesulfonate substituents, respectively.

Considering this, **A1** host is roughly twice (~2.72 Å) as deep as C_{ethyl}-2-H-resorcinarene. The d_1 and d_2 distances are calculated between closest O···O atoms of the opposite sulfonate groups and represents the portal of the **A1** (Table 1) in vase-conformation, which is evidently smaller than that of a wider-mouth C_{ethyl}-2-H-resorcinarene calculated from distances of upper-rim 2-position carbon atoms (~7.45/9.37 Å).

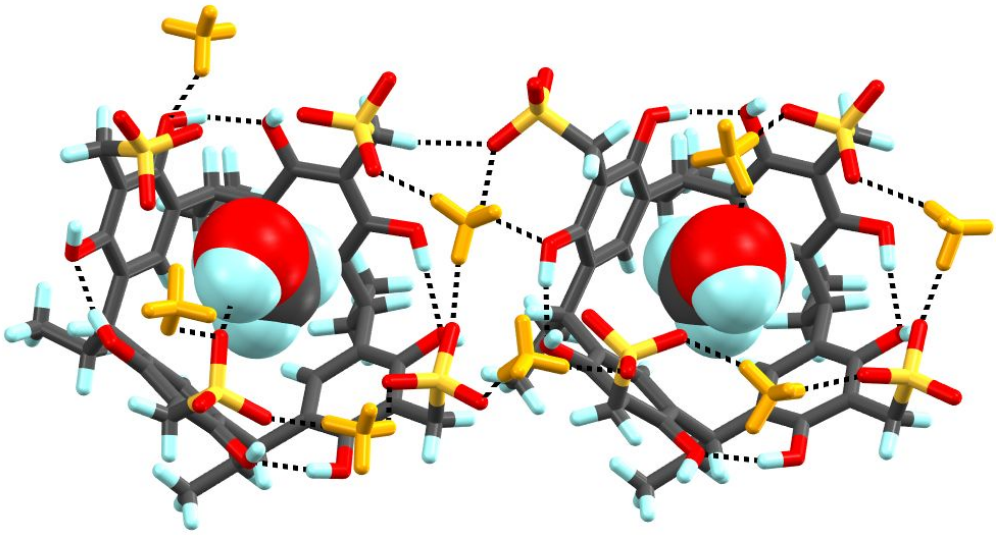

Figure 4. X-Ray crystal structure of **B1**@**A1** in stick model. Ammonium ions are orange color sticks and the dashed lines represent hydrogen bonds.

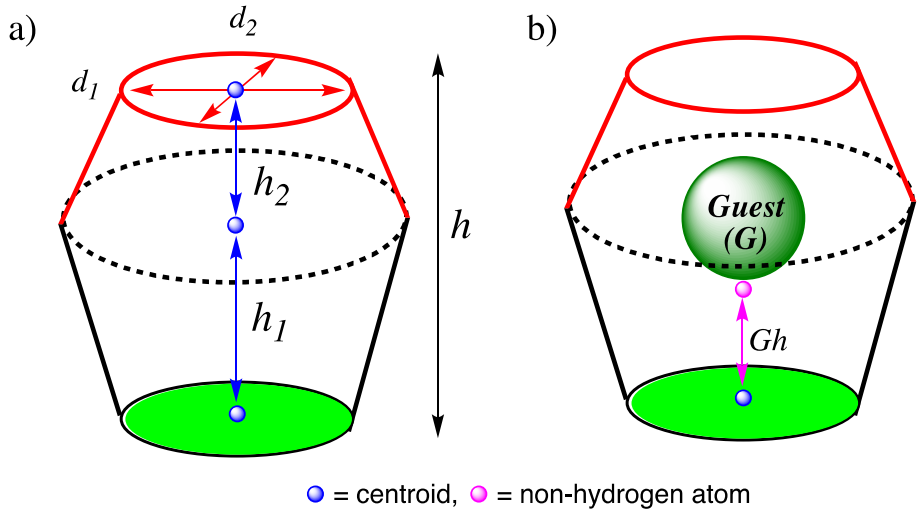

Figure 5. Pictorial representation of **A1** structure in vase conformation displaying dimensions of host a), and position of the *endo*-guest from the lower-rim centroid b).

Table 2. Dimensions of host **A1** in vase conformation derived from X-ray crystal structures.

Name	SO_3 conformation	h_1/h_2 (*ca.* Å)	h (*ca.* Å)	d_1/d_2 (*ca.* Å)	*Gh* (*ca.* Å)
B1@A1	4-*in*	2.15/2.70	4.85	6.51/8.35	2.90
	3-*in*-1-*out*[a]	2.13/2.34	4.47	6.68/9.34	2.88
B2@A1	4-*in*	2.13/2.72	4.85	7.14/7.59	3.39
	2-*in*-2-*out*[a]	2.18/2.63	4.81	8.72/8.98	3.40
B2@A1_1	4-*in*	2.10/2.64	4.74	8.0/8.14	3.55
B8@A1	3-*in*-1-*out*[a]	1.98/2.79	4.77	6.39/10.31	2.67
B9@A1	3-*in*-1-*out*[a]	1.96/2.73	4.69	7.53/10.33	2.94

[a]The values are presented for reference purpose only, for more information see SI

Complex **B2@A1** is a 2-D coordination polymer, $[2(\mathbf{A1})^{4-} \cdot 3(\mathbf{B2})^{+} \cdot 5Na^{+}]_n$, the single crystals were prepared by mixing 1:10 molar ratio of **A1** and **B2**. The asymmetric unit contains two host molecules, three $\mathbf{B2}^{+}$ and five sodium ions coordinating to sulfonate oxygen atoms. The two **A1**

cavities are filled with two **B2**$^{+}$, respectively, while the third **B2**$^{+}$ is *exo*-cavity. Sulfonate groups of one of the hosts in **B2**@**A1** are in 4-*in* conformation while surprisingly a 2-*in*-2-*out* conformation is observed for the other host molecule as shown in Figure 6. Compared to the methanol solvent in **B1**@**A1**, the bulkier and tetrahedral geometry *endo*-**B2**$^{+}$ guest shows larger *Gh* values 3.39 Å (4-*in*) and 3.40 Å (2-*in*-2-*out*). The -CH_3 groups are stabilized both by C−H···π and C−H···O interactions with their corresponding overall distances range from *ca.* 2.622 to 2.893 Å and 2.462 to 2.706 Å. The d_1 and d_2 distances of 4-*in* of **B2**@**A1** are larger compared to 4-*in* of **B1**@**A1** suggesting that the host cavity opened up to accommodate the additional stabilizing attractive electrostatic interactions between negatively charged sulfonate groups and electron-deficient -CH_3 groups of **B2**$^{+}$.

The formation of different conformations in **B2**@**A1** can be related to the electrical neutrality of the structure where the negatively charged sulfonate groups are compensated by positively charged **B2**$^{+}$ and sodium ions. Therefore, the combination of cation-anion interactions between **B2**$^{+}$ and -SO_3^-, high affinity O−Na coordination bonds, and crystal packing forces all affect the different host conformations. Fortunately, to better understand the electrostatic cation-anion interactions between **B2**$^{+}$ and -SO_3^- groups in a sodium free-lattice, the success of **B2**@**A1** **_1** prepared in 1:25 molar ratio of **A1** and **B2** resulted in a fully desalinated H-G complex of the type, [(**A1**)$^{4-}$·4(**B2**)$^{+}$]. The asymmetric unit contains a **A1**$^{4-}$ molecule and the four negative charges that are counterbalanced by four **B2**$^{+}$ guests. One of them is inside the cavity and the other three outside. The vase conformation of **A1**$^{4-}$ is shown in Figure 6b, and *Gh* of the *endo*-**B2**$^{+}$ at 3.55 Å is *ca.* 0.16 Å larger compared to *endo*-**B2**$^{+}$ of **B2**@**A1**. This reflects from larger d_1 and d_2 distances suggesting that the *endo*-**B2**$^{+}$ is stabilized by sulfonate groups electrostatic interactions.

Remarkably, in the 3-D crystal packing, each $\mathbf{A1}^{4-}$ were surrounded by the four *exo*-$\mathbf{B2}^{+}$ which is further proof that there are attractive cation-anion interactions between sulfonate groups and $\mathbf{B2}^{+}$.

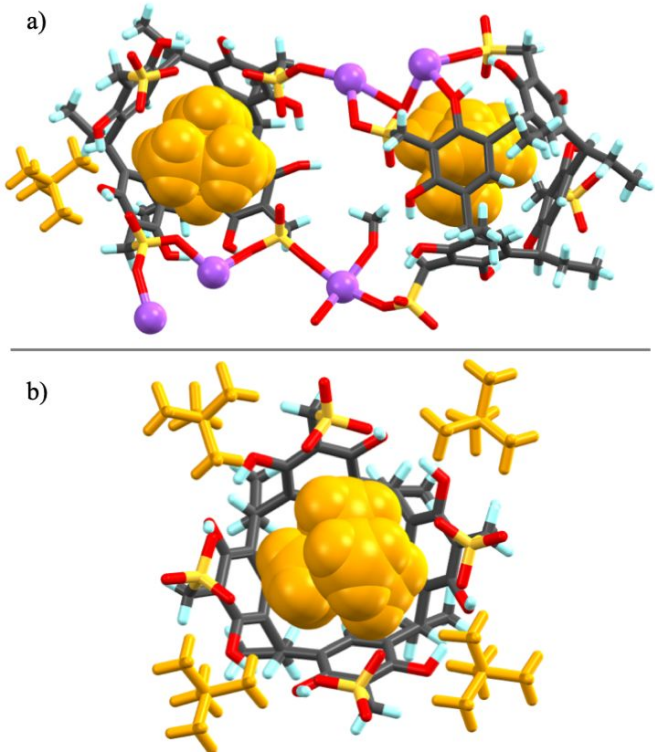

Figure 6. X-Ray crystal structure of **B2@A1** a), and **B2@A1_1** b). Representation: *exo*-$\mathbf{B2}^{+}$ are in orange color sticks and *endo*-$\mathbf{B2}^{+}$ in CPK models. Host are sticks and sodium in ball & stick.

Complex **B8@A1**, prepared in 1:10 molar ratio of **A1** and **B8**, crystallizes in the triclinic space group *P*-1. The asymmetric unit contains a host and the charge is balanced by one $\mathbf{B8}^{+}$ and three sodium ions suggesting desalination of one sodium iodide during the H-G complexation. The host displays 3-*in*-1-*out* sulfonate group conformation with regards to cavity, and the aromatic part of $\mathbf{B8}^{+}$ is inside the cavity manifesting the ${}_{G}(C{-}H)\cdots(\pi)_{H}$ interactions between guest and host at distances *ca*. 2.752 to 2.859 Å rather than the *N*-methyl group. This agrees with the ^{1}H NMR solution spectra. In the packing structure, the repeating unit $[(\mathbf{A1})^{4-}\cdot(\mathbf{B8})^{+}\cdot 3Na^{+}\cdot 2(CH_3OH)]_n$

extends in 2-D layers with sulfonate groups coming together in head-to-head fashion and coordinating sodium ions to give capsule-like motifs (Figure 7a and S15-16). The two host molecules of the capsule are displaced with respect to each other instead of a ″perfect″ molecular capsule arrangement and the distance between their lower-rim centroids is *ca.* 12.0 Å (Figure S19). The shorter dimensions of **B8**$^+$ could be responsible for lower *Gh* value (*ca.* 2.67 Å) and slipped capsular arrangement in bilayer structures. The two **B8**$^+$ molecules per capsule are positioned to the opposite corners of the host facilitating C−H···O interactions between acidic C2-protons/*N*−CH_3 groups and sulfonate oxygen atoms ranging from *ca*. 2.183 to 2.868 Å, with the shortest contact distance is found between guest acidic C2-proton and sulfonate oxygen. Additionally, weak $\pi\cdots\pi$ interactions (*ca.* 3.305 Å) were present between *endo*-**B8**$^+$ and host aromatic rings.

The complex **B9**@**A1** crystallized from methanolic solution in 1:10 molar ratio was determined in the triclinic space group *P*-1. While **B9**@**A1** forms a 2-D bilayer coordination polymer by capsular arrangement structurally similar to **B8**@**A1**, the capsular-like cavities contain only one *endo*-**B9**$^+$ guest disordered over two positions with 50:50 occupancy (Figure 7b and S17-18). This complements the ^{1}H NMR results which shows the *N*-CH_3 group to be predominantly in the cavity. The guest is located almost in the center of the capsule presumably to avoid the steric effects. Therefore, the *endo*-**B9**$^+$ mainly displays C−H···π contacts with the aromatic ring of one of the hosts at distances between *ca*. 2.668 and 3.108 Å, the shortest contact being the C−H···π(centroid) and few C−H···O interactions (*ca*. 2.887 and 2.987 Å). The **A1** once again demonstrates the 3-*in*-1-*out* conformation here. Although the centroid-to-centroid lower-rim distances (*ca.* 12.0 Å) of the capsule is the same as in **B8**@**A1**, surprisingly, the longer guest **B9**$^+$ *Gh* value (2.94 Å) is similar to **B8**$^+$.

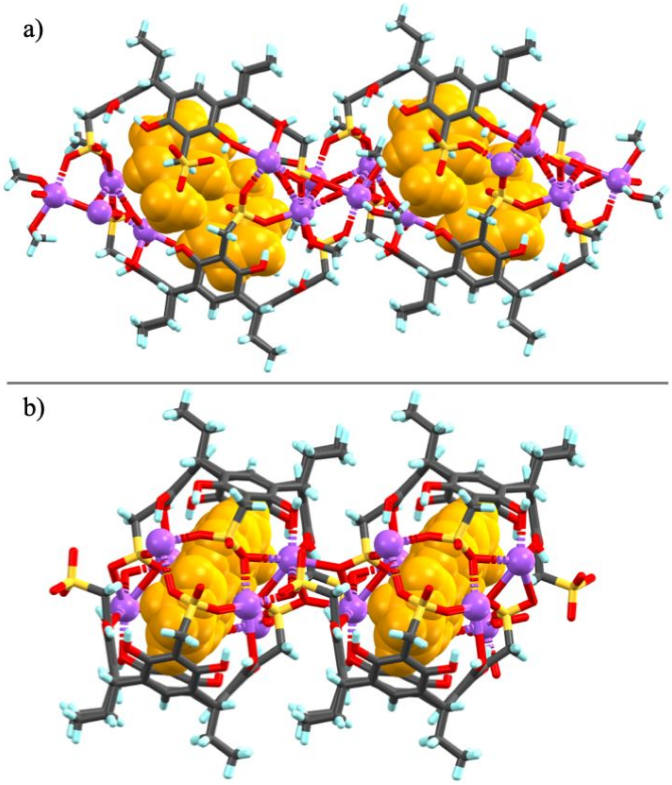

Figure 7. X-Ray crystal structure of **B8**@**A1** a), and **B9**@**A1** b). Representation: *endo*- **B8**$^{+}$ and **B9**$^{+}$ are in orange CPKs, host are stick and sodium in ball & stick.

Computational studies

In resorcinarene H-G chemistry, C−H···π contacts are important motifs for the molecular recognition of ammonium cations, aromatic and N-heterocycle compounds.[1] The success of *endo*-complexation selectivity depends on H-bonding interactions, steric, electronic, H-G complementarity, and pre-organization of the participating host and guest compounds. The H-G interactions of Type 1 tetrasulfonatoresorcinarenes have been previously studied computationally towards insulin monomers using molecular docking and molecular dynamics simulations[52] and towards osteoporosis inhibitor drug zoledronate using BLYP-GGA/DZP DFT calculations[53]. Here,

to qualitatively address the interactions and energetic trends in resorcinarene H-G complexes DFT calculations were carried out on model sodium free sulfonatomethyleneresorcinarene host with -CH_3 groups in the lower-rim (**A3**)$^{4-}$ and its selected complexes to save computational time. The **A1** H-G crystal structures already illustrated that sulfonatomethylene groups can adopt several conformations in crystal structures. Optimizations of the free host (**A3**)$^{4-}$ anion showed the minimum structure of the anion to be 4-*out* conformation where negative charge on the O-atoms of sulfonate groups is evenly distributed (Figure 8). In the 4-*in* conformation, the sulfonate groups are inwardly directed towards the center of the cavity and the negative charge concentrates on the O-atoms that are closest to the center of the cavity. The repulsion between negative charge causes the sulfonate groups to move away from the center opening the cavity wider compared to vase conformations in the X-ray crystal structure geometries of **A1** and lowers the stability of the 4-*in* structure resulting in +39 kcal mol^{-1} higher relative enthalpy compared to that of 4-*out* conformation. In addition, four other conformations between 4-*in* and 4-*out* extremes were found for (**A3**)$^{4-}$ with relative enthalpies of +28 (3-*in*-1-*out*), +17 (2-*in*-2-*out*′), +16 (2-*in*-2-*out*′′), and +8 kcal mol^{-1} (1-*in*-3-*out*) compared to 4-*out* and structures shown in the Supporting Information Figure S20.

In H-G systems, the relative stabilities of resorcinarene conformations are strongly affected by the interactions from the *endo*-guests inside the cavity that favor directing at least some of the sulfonate groups inside the ring to maximize the H-G interactions. For example, the H-G interactions between **B2**$^{+}$ H-atoms and sulfonate O-atoms stabilize the 4-*in* conformation more than the 4-*out* conformation making their calculated complex structures equally stable as shown in Figure 9. In 4-*in* and 4-*out* complex conformations, the **B2**$^{+}$ resides at the center of the cavity

and the H-G interactions are not optimal whereas in 3-*in*-1-*out* and 2-*in*-2-*out* conformations the **B2**$^{+}$ interacts with three and two sulfonate groups forming more stable complexes in the gas phase with relative enthalpies of –6 and –8 kcal mol^{-1}, respectively, albeit the differences are not large. This situation is also reflected in X-ray crystal structures, **B2@A1** and **B2@A1_1**, where structures corresponding to 4-*in* and 2-*in*-2-*out* conformations of (**A1**)$^{4-}$ have been found. The binding enthalpy in the gas phase for the most stable **B2**$^{+}$@(**A3**)$^{4-}$ structure 2-*in*-2-*out* is –221 kcal mol^{-1}. The calculated binding enthalpy is high compared to for example the binding energy reported for complex of protonated tetrasulfonatoresorcinarene and molecular zoledronate –32 kcal mol–1,[53] but the difference can be explained by the high negative charge of the host anion that has not been compensated by other cations in the calculated structures here.

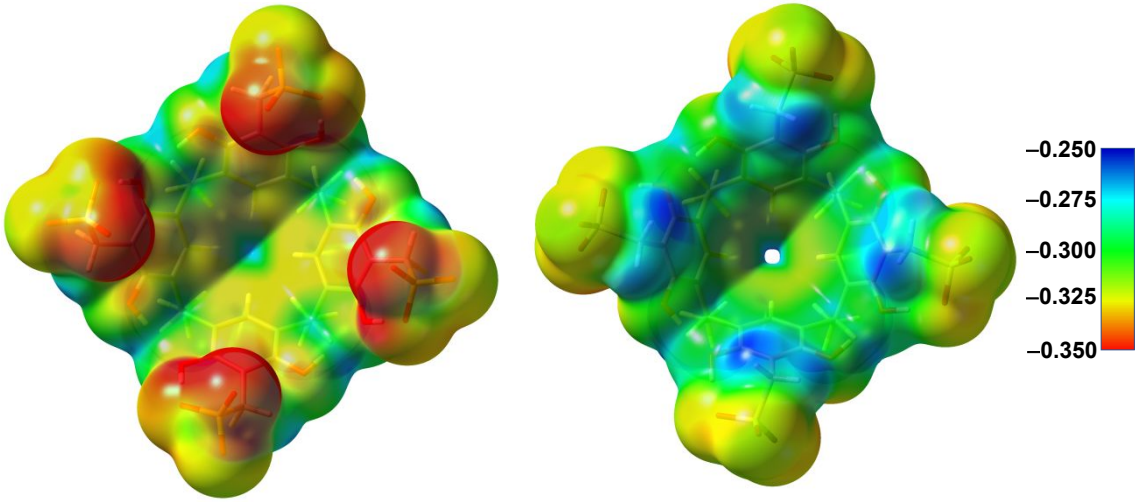

Figure 8. Electrostatic potential projected on the 0.001 au electron density surface of model host (**A3**)$^{4-}$ anion conformations, 4-*in* (left-side) and 4-*out* (right-side).

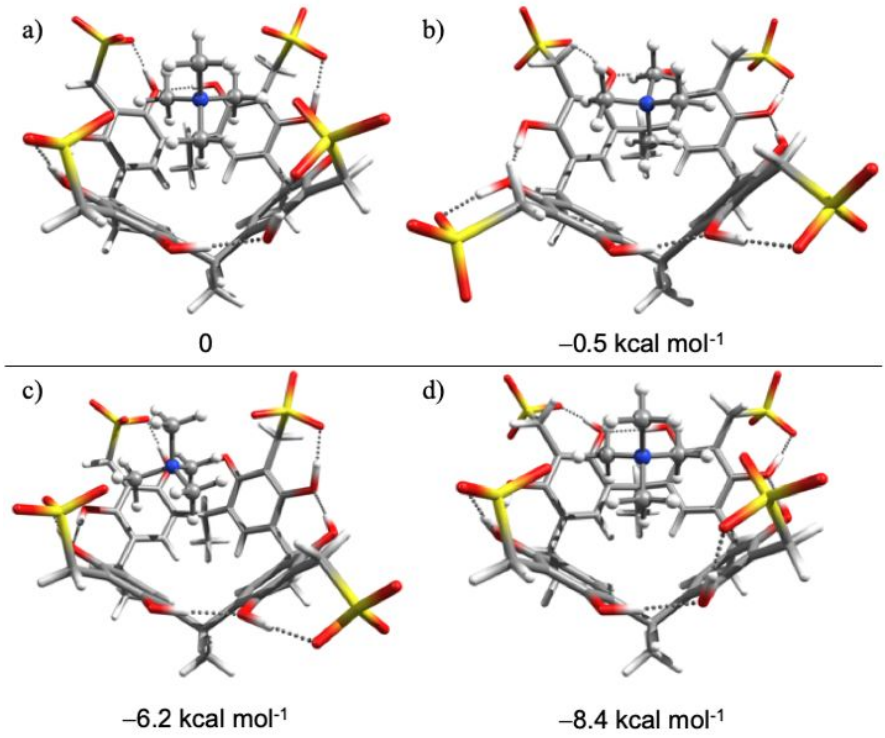

Figure 9. Structures of model $\mathbf{B2}^{+}$@$(\mathbf{A3})^{4-}$ host-guest complex conformations optimized at PBE0-D3/def-TZVP level of theory.

To qualitatively access the relative strengths of different types of H-G interactions alternative conformations of $\mathbf{B3}^{+}$@$(\mathbf{A3})^{4-}$ and $\mathbf{B5}^{+}$@$(\mathbf{A3})^{4-}$ *endo*-complexes exhibiting *N*-methyl, *N*-butyl, *N*-ethyl and *N*-phenyl guest to host interactions were optimized. First the analysis of $\mathbf{B3}^{+}$ and $\mathbf{B5}^{+}$ electrostatic surfaces shows the highest positive surface charges on H-atoms attached to the nitrogen atoms and the surface charges becoming less positive further away from the nitrogen atoms (Figure 10). From electrostatic potential analyses it would be expected that in the most stable H-G systems the interactions between the highest negative charge concentrations of $(\mathbf{A3})^{4-}$ anion and the highest positively charged sites on $\mathbf{B3}^{+}$ and $\mathbf{B5}^{+}$ cations would be maximized. For the H-G system optimizations, two starting geometries with different *endo*-guest functional groups pointing inside the host cavity were considered to determine the favored orientation of the *endo*-

guest and the relative stabilities of the formed interactions (Figure 11). In complex **B3**$^{+}$@(**A3**)$^{4-}$, the methyl end fits into the cavity and at the same time optimal N−H···O interactions are formed between H-atoms bound to nitrogen atom and sulfonate groups (**B3**$^{+}$@(**A3**)$^{4-}$_**a**, Figure 11a). On the other hand, the less positively charged longer butyl chain of **B3**$^{+}$, which does not fit inside the cavity, resides on top of the resorcinarene cavity in the optimized structure (**B3**$^{+}$@(**A3**)$^{4-}$_**b**, Figure 11b). The better fit between (**A3**)$^{4-}$ and **B3**$^{+}$ in structure **B3**$^{+}$@(**A3**)$^{4-}$_**a** also results in more tight H-G binding with ΔH = –265 kcal mol^{-1} compared to –258 kcal mol^{-1} in **B3**$^{+}$@(**A3**)$^{4-}$_**b**. In **B5**$^{+}$@(**A3**)$^{4-}$ complex, the guest inclusion phenomenon is similar to **B3**$^{+}$@(**A3**)$^{4-}$_**a** that is the ethyl end of **B5**$^{+}$ best fits into the cavity as the -NH_2 group H-bonds to sulfonate O-atoms. Although the phenyl ring is capable of exerting π-delocalization of the positive charge on the N-atom to render the aromatic C−H protons more electron-deficient, the phenyl ring of **B5**$^{+}$ does not fit into the cavity and is parallel to cavity like a lid on vase in the optimized structure **B5**$^{+}$@(**A3**)$^{4-}$_**b** (Figure 11d). However, in contrast to relative stabilities of **B3**$^{+}$@(**A3**)$^{4-}$ structures, the **B5**$^{+}$@(**A3**)$^{4-}$_**b** is similar in stability to **B5**$^{+}$@(**A3**)$^{4-}$_**a** structure with binding enthalpies of –264 and –263 kcal mol^{-1}, respectively. The stability of the **B5**$^{+}$@(**A3**)$^{4-}$_**b** structure is likely to arise from the C−H···π contacts between the cationic phenyl ring and the negatively charged sulfonate groups. Given the small stability difference between **B5**$^{+}$@(**A3**)$^{4-}$ structures the guest solvent interactions or charge compensation by other ions in solution can easily change the stability order to that observed by ^{1}H NMR measurements in solution.

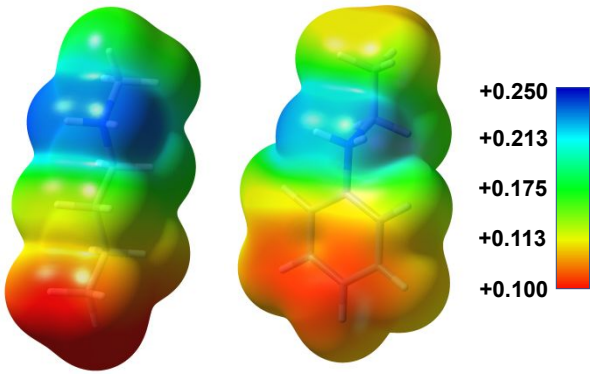

Figure 10. Electrostatic potentials of **B3**$^{+}$ and **B5**$^{+}$ projected on the 0.001 au electron density surfaces.

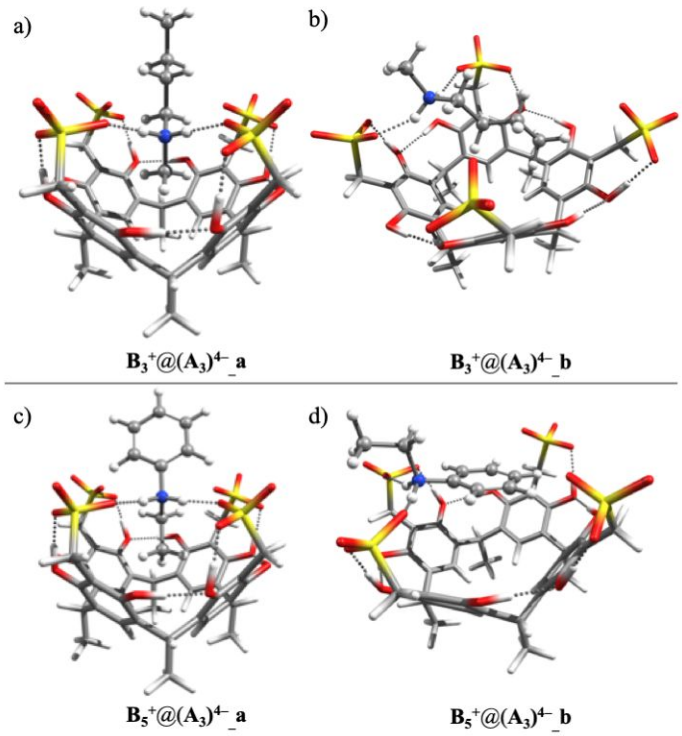

Figure 11. Structures of model H-G complexes of a) **B3**$^{+}$**@(A3)**$^{4-}$**_a**, b) **B3**$^{+}$**@(A3)**$^{4-}$**_b**, c) **B5**$^{+}$**@(A3)**$^{4-}$**_a**, and d) **B5**$^{+}$**@(A3)**$^{4-}$**_b** optimized at PBE0-D3/def-TZVP level of theory. The black dashed lines are H-bond interactions.

CONCLUSIONS

A comprehensive solution ^{1}H NMR study of the H-G complexation process between $C_{\mathbf{R}}$-tetrasodiumsulfonatomethyleneresorcinarene (**R** = ethyl and hexyl) and ammonium halides was carried out in a hydrogen bond competing solvent, MeOH-d_4. Comparison of the complexation behavior of more flexible lower-rim ethyl substituted host to hexyl substituted host emphasized importance of retaining resorcinarene flexibility in order to achieve effective binding of guests by host. In solution, despite the upper-rim host cavity being surrounded by hydrogen bond competing sulfonate oxygen atoms, the C−H···π contacts between guest and host are the key driving non-covalent interactions for 14 out of 16 observed *endo*-complexes. The exception being for *N*-butyl-*N*-benzylammonium cation, where the hydrogen bonding between -NH_2 and sulfonate oxygens restricts both *N*-butyl and *N*-benzyl groups from *endo*-complexation. Isothermal calorimetry titrations were carried out to quantify association constants. The binding was spontaneous at 303 K. The highest binding constant observed for tetramethylammonium cation guest (K_a = 909.10 M^{-1}) reflects the perfect size match between the host and guest. Flexibility and size mis-match were also highlighted with lower binding constants of some of the guests. X-ray crystal structures revealed that the methylenesulfonate groups offer an extended cavity space, when all the four sulfonate groups are inwardly directed into the cavity. The host conformation evidence the increased stabilization of *endo*-guests by $SO_3\cdots(C-H)_{guest}$ contacts in addition to existing well-known *endo*- C−H···π interactions. In our host-guest study, the validation of the conformations of tetrasulfonatomethylene groups with respect to host cavity in a 4-*in*, 3-*in*-1-out, and 2-*in*-2-*out* were realized by X-ray diffraction analysis. DFT computational studies were used to examine the relative stabilities of these and other not experimentally observed conformations of the host anion. The conformational flexibility of sulfonate groups and the existence of several conformations in

the gas-phase and in solid-state structures is related to the intramolecular hydrogen bonding between hydroxyl groups and sulfonate oxygens that can kinetically stabilize the higher energy conformations. This work offers more fundamental insights into the unique properties of tetrasulfonatomethylene resorcinarenes and their potential as receptors for a variety of cationic guests in highly competitive solvent.

EXPERIMENTAL SECTION

The solvents used for synthesis, ^{1}H NMR and ITC experiments, and crystallization experiments were reagent grade and are used as received without further purification. Hosts **A1** and **A2**,[37] and **B3** - **B9**[54] were synthesized by following the literature methods. Guest **B1** and **B2** were purchased from Sigma Aldrich. ^{1}H NMR spectra were recorded on a Bruker Avance DRX 500 and 400 spectrometers. ITC measurements were performed using VP-ITC instrument made by MicroCal. Single-crystal X-ray data were measured using a dual-source Rigaku SuperNova diffractometer equipped with an Atlas detector and an Oxford Cryostream cooling system, using either mirror-monochromated Cu-K_α (λ = 1.54184 Å; for **B1**@**A1**, **B2**@**A1** and **B2**@**A1_1**) or mirror-monochromated Mo-K_α radiation (λ = 0.71073 Å; for **B8**@**A1** and for **B9**@**A1**). Data collection and reduction for all complexes were performed using the program *CrysAlisPro*[55] and Gaussian face-index absorption correction method was applied.[55] All structures were solved with Direct Methods or Patterson synthesis (*SHELXS*)[56] and refined by full-matrix least squares based on F^2 using *SHELXL*-2013.[56] Single-crystal X-ray data experimental details and CCDC numbers are given in Supporting Information.

Structures of complexes, host anions and guest cations were fully optimized with Gaussian 16 program package[59] using PBE0 hybrid density functional[60–63] and Ahlrichs' small triple-ζ valence

quality basis set def-TZVP[64] combined with Grimme's empirical D3BJ correction[65] to treat the dispersion forces. Structure of the host **(A1)$^{4-}$** anion in **B2@A1_1** crystal structure was used as a starting point for the optimization of 4-*in* conformation of **(A3)$^{4-}$** anion by replacing the lower rim -C_2H_5 groups with -CH_3 groups. Starting points for the optimizations of other host conformations and H-G structures were obtained by modifying the orientation of the sulfonato groups and placing guest cations in different orientations in the middle of the host ring. Host-guest binding enthalpies were calculated as the enthalpy difference between the complex structures and the minimum energy conformations of free host anions and guest cations.

ASSOCIATED CONTENT

Supporting Information. The Supporting Information is available free of charge on the ACS Publication website at DOI: XXXXX. X-Ray experimental details and computational data are included in the Supporting Information.

ACKNOWLEDGMENT

The authors gratefully acknowledge financial support from Oakland University, MI, USA, the Academy of Finland (RP: grant no. 298817) and the University of Jyväskylä. The Finnish Grid and Cloud Infrastructure (urn:nbn:fi:research-infras-2016072533) and Prof. H. M. Tuononen (University of Jyväskylä) are acknowledged for providing computational resources.

REFERENCES

(1) Sliwa, W.; Kozlowski, C. *Calixarenes and Resorcinarenes*; Wiley, 2009.

(2) Schneider, H.-J.; Schneider, U. The Host-Guest Chemistry of Resorcinarenes. *J. Incl. Phenom. Mol. Recognit. Chem.* **1994**, *19*, 67–83.

(3) Timmerman, P.; Verboom, W.; Reinhoudt, D. N. Resorcinarenes. *Tetrahedron* **1996**, *52*,

2663–2704.

(4) Jasat, A.; Sherman, J. C. Carceplexes and Hemicarceplexes. *Chem. Rev.* **1999**, *99*, 931–968.

(5) Neri, P.; Sessler, J. L.; Wang, M. X. *Calixarenes and Beyond*; Springer International Publishing, 2016.

(6) Böhmer, V. Calixarenes, Macrocycles with (Almost) Unlimited Possibilities. *Angew. Chemie Int. Ed. English* **1995**, *34*, 713–745.

(7) Gramage-Doria, R.; Armspach, D.; Matt, D. Metallated Cavitands (Calixarenes, Resorcinarenes, Cyclodextrins) with Internal Coordination Sites. *Coord. Chem. Rev.* **2013**, *257*, 776–816.

(8) Kobayashi, K.; Yamanaka, M. Self-Assembled Capsules Based on Tetrafunctionalized Calix[4]Resorcinarene Cavitands. *Chem. Soc. Rev.* **2015**, *44*, 449–466.

(9) Zhou, J.; Chen, M.; Diao, G. Assembling Gold and Platinum Nanoparticles on Resorcinarene Modified Graphene and Their Electrochemical Applications. *J. Mater. Chem. A* **2013**, *1*, 2278–2285.

(10) Shen, M.; Sun, Y.; Han, Y.; Yao, R.; Yan, C. Strong Deaggregating Effect of a Novel Polyamino Resorcinarene Surfactant on Gold Nanoaggregates under Microwave Irradiation. *Langmuir* **2008**, *24*, 13161–13167.

(11) Sun, Y.; Yao, Y.; Yan, C.-G.; Han, Y.; Shen, M. Selective Decoration of Metal Nanoparticles inside or Outside of Organic Microstructures via Self-Assembly of Resorcinarene. *ACS Nano* **2010**, *4*, 2129–2141.

(12) Tripp, S. L.; Pusztay, S. V; Ribbe, A. E.; Wei, A. Self-Assembly of Cobalt Nanoparticle Rings. *J. Am. Chem. Soc.* **2002**, *124*, 7914–7915.

(13) Liu, W.; Yang, H.; Wu, W.; Gao, H.; Xu, S.; Guo, Q.; Liu, Y.; Xu, S.; Cao, S. Calix[4]Resorcinarene-Based Branched Macromolecules for All-Optical Photorefractive Applications. *J. Mater. Chem. C* **2016**, *4*, 10684–10690.

(14) Xu, S.; Fang, C.; Wu, Y.; Wu, W.; Guo, Q.; Zeng, J.; Wang, X.; Liu, Y.; Cao, S. Photorefractive Hyper-Structured Molecular Glasses Constructed by Calix[4]Resorcinarene Core and Carbazole-Based Methine Nonlinear Optical Chromophore. *Dye. Pigment.* **2017**, *142*, 8–16.

(15) Beyeh, N. K.; Díez, I.; Taimoory, S. M.; Meister, D.; Feig, A. I.; Trant, J. F.; Ras, R. H. A.; Rissanen, K. High-Affinity and Selective Detection of Pyrophosphate in Water by a Resorcinarene Salt Receptor. *Chem. Sci.* **2018**, *9*, 1358–1367.

(16) Haines, S. R.; Harrison, R. G. Novel Resorcinarene-Based PH-Triggered Gelator. *Chem. Commun.* **2002**, 2846–2847.

(17) Li, N.; Harrison, R. G.; Lamb, J. D. Application of Resorcinarene Derivatives in Chemical Separations. *J. Incl. Phenom. Macrocycl. Chem.* **2014**, *78*, 39–60.

(18) Gambaro, S.; La Manna, P.; De Rosa, M.; Soriente, A.; Talotta, C.; Gaeta, C.; Neri, P. The Hexameric Resorcinarene Capsule as a Brønsted Acid Catalyst for the Synthesis of Bis(Heteroaryl)Methanes in a Nanoconfined Space. *Front. Chem.* **2019**, *7*, 687.

(19) Zhang, Q.; Catti, L.; Tiefenbacher, K. Catalysis inside the Hexameric Resorcinarene Capsule. *Acc. Chem. Res.* **2018**, *51*, 2107–2114.

(20) Pappalardo, A.; Puglisi, R.; Trusso Sfrazzetto, G. Catalysis inside Supramolecular Capsules: Recent Developments. *Catalysts* **2019**, *9,* 630.

(21) La Manna, P.; Talotta, C.; Floresta, G.; De Rosa, M.; Soriente, A.; Rescifina, A.; Gaeta, C.; Neri, P. Mild Friedel–Crafts Reactions inside a Hexameric Resorcinarene Capsule: C−Cl Bond Activation through Hydrogen Bonding to Bridging Water Molecules. *Angew. Chem. Int. Ed.* **2018**, *57*, 5423–5428.

(22) Kobayashi, K.; Asakawa, Y.; Kikuchi, Y.; Toi, H.; Aoyama, Y. CH-.Pi. Interaction as an Important Driving Force of Host-Guest Complexation in Apolar Organic Media. Binding of Monools and Acetylated Compounds to Resorcinol Cyclic Tetramer as Studied by Proton NMR and Circular Dichroism Spectroscopy. *J. Am. Chem. Soc.* **1993**, *115*, 2648–2654.

(23) Mahalakshmi, L.; Das, P. P.; Guru Row, T. N. Self Assembly of C-Methyl Resorcin[4]Arene with Coumarin and Thiocoumarin: A Nanotubular Array with a near Perfect Lock and Key Fit. *J. Chem. Sci.* **2008**, *120*, 39–44.

(24) Ma, B.-Q.; Coppens, P. Symmetry Mismatching as a Tool in the Synthesis of Complex Supramolecular Solids with Multiple Cavities. *Cryst. Growth Des.* **2004**, *4*, 211–213.

(25) Ma, B.-Q.; Zhang, Y.; Coppens, P. Multiple Structures in Supramolecular Solids: Benzophenone Embedded in Three Different C-Methylcalix[4]Resorcinarene/Bipyridine Frameworks. *Cryst. Growth Des.* **2001**, *1*, 271–275.

(26) Pfeiffer, C. R.; Atwood, S. G.; Samadello, L.; Atwood, J. L. Investigating Properties and Trends of Cocrystals Composed of Pyrogallol[4]Arenes and Anthracene-Based Fluorescent Probes. *Cryst. Growth Des.* **2015**, *15*, 2958–2978.

(27) Atwood, J. L.; Szumna, A. Cation–Pi Interactions in Neutral Calix[4]Resorcinarenes. *J. Supramol. Chem.* **2002**, *2*, 479–482.

(28) Barnes, C. L.; Bosch, E. Self-Assembly of C-Methyl Calix[4]Resorcinarene with 5,5'-Bipyrimidine. *J. Chem. Crystallogr.* **2007**, *37*, 783–786.

(29) Jiang, S.; Patil, R. S.; Barnes, C. L.; Atwood, J. L. Application of Cocrystallization for the Separation of C-Ethylresorcin[6]Arene from C-Ethylresoricn[4]Arene. *Cryst. Growth Des.* **2017**, *17*, 4060–4063.

(30) Patel, M. B.; Valand, N. N.; Modi, N. R.; Joshi, K. V; Harikrishnan, U.; Kumar, S. P.; Jasrai, Y. T.; Menon, S. K. Effect of P-Sulfonatocalix[4]Resorcinarene (PSC[4]R) on the Solubility and Bioavailability of a Poorly Water Soluble Drug Lamotrigine (LMN) and Computational Investigation. *RSC Adv.* **2013**, *3*, 15971–15981.

(31) Hoskins C, Papachristou A, Ho TMH, Hine J, C. A. Investigation into Drug Solubilisation Potential of Sulfonated Calix[4] Resorcinarenes. *J. Nanomedicine Nanotechnol.* **2016**, *7*, 370.

(32) Mustafina, A. R.; Fedorenko, S. V; Makarova, N. A.; Kazakova, E. K. H.; Bazhanova, Z.

G.; Kataev, V. E.; Konovalov, A. I. The Inclusion Properties of a New Watersoluble Sulfonated Calix[4]Resorcinarene towards Alkylammonium and N-Methylpyridinium Cations. *J. Incl. Phenom. Macrocycl. Chem.* **2001**, *40*, 73–76.

(33) Sanabria, E.; Esteso, M. Á.; Vargas, E.; Maldonado, M. Experimental Comparative Study of Solvent Effects on the Structure of Two Sulfonated Resorcinarenes. *J. Mol. Liq.* **2018**, *254*, 391–397.

(34) Sanabria, E.; Esteso, M. Á.; Pérez-Redondo, A.; Vargas, E.; Maldonado, M. Synthesis and Characterization of Two Sulfonated Resorcinarenes: A New Example of a Linear Array of Sodium Centers and Macrocycles. *Molecules* **2015**, *20*, 9915–9928.

(35) Ede, J. A.; Cragg P. J.; Sambrook, M. R. Comparison of Binding Affinities ofWater-Soluble Calixarenes with the Organophosphorus Nerve Agent Soman (GD) and Commonly-Used Nerve Agent Simulants, *Molecules* **2018**, *23*, 207.

(36) Galindres, D. M.; Ribeiro, A. C. F.; Valente, A. J. M.; Esteso, M. A.; Sanabria, E.; Vargas, E. F.; Verissimo, L. M. P.; Leaist, D. G. Ionic Conductivities and Diffusion Coefficients of Alkyl Substituted Sulfonated Resorcinarenes in Aqueous Solutions. *J. Chem. Thermodyn.* **2019**, *133*, 223–228.

(37) Kazakova, E. K.; Makarova, N. A.; Ziganshina, A. U.; Muslinkina, L. A.; Muslinkin, A. A.; Habicher, W. D. Novel Water-Soluble Tetrasulfonatomethylcalix[4]Resorcinarenes. *Tetrahedron Lett.* **2000**, *41*, 10111–10115.

(38) Syakaev, V. V; Kazakova, E. K.; Morozova, J. E.; Shalaeva, Y. V; Latypov, S. K.; Konovalov, A. I. Guest Controlled Aggregation of Amphiphilic Sulfonatomethylated Calix[4]Resorcinarenes in Aqueous Solutions. *J. Colloid Interface Sci.* **2012**, *370*, 19–26.

(39) Shalaeva, Y. V; Morozova, J. E.; Syakaev, V. V; Kazakova, E. K.; Ermakova, A. M.; Nizameev, I. R.; Kadirov, M. K.; Konovalov, A. I. Supramolecular Nanoscale Systems Based on Amphiphilic Tetramethylensulfonatocalix[4]Resorcinarenes and Cationic Polyelectrolyte with Controlled Guest Molecule Binding. *Supramol. Chem.* **2017**, *29*, 278–289.

(40) Amirov, R. R.; Nugaeva, Z. T.; Mustafina, A. R.; Fedorenko, S. V; Morozov, V. I.; Kazakova, E. K.; Habicher, W. D.; Konovalov, A. I. Aggregation and Counter Ion Binding Ability of Sulfonatomethylcalix[4]Resorcinarenes in Aqueous Solutions. *Colloids Surfaces A Physicochem. Eng. Asp.* **2004**, *240*, 35–43.

(41) Guo, D-S.; Liu, Y.; Supramolecular Chemistry of *p*-Sulfonatocalix[*n*]arenes and Its Biological Applications. *Acc. Chem. Res.* **2014**, *47*, 1925-1934

(42) Hong, M.; Zhang, Y.-M.; Liu, Y. Selective Binding Affinity between Quaternary Ammonium Cations and Water-Soluble Calix[4]Resorcinarene. *J. Org. Chem.* **2015**, *80*, 1849–1855.

(43) Kobayashi, K.; Asakawa, Y.; Kato, Y.; Aoyama, Y. Complexation of Hydrophobic Sugars and Nucleosides in Water with Tetrasulfonate Derivatives of Resorcinol Cyclic Tetramer Having a Polyhydroxy Aromatic Cavity: Importance of Guest-Host CH-.Pi. Interaction. *J. Am. Chem. Soc.* **1992**, *114*, 10307–10313.

(44) Kashapov, R. R.; Pashirova, T. N.; Kharlamov, S. V; Ziganshina, A. Y.; Ziltsova, E. P.; Lukashenko, S. S.; Zakharova, L. Y.; Habicher, W. D.; Latypov, S. K.; Konovalov, A. I. Novel Self-Assembling System Based on Resorcinarene and Cationic Surfactant. *Phys. Chem. Chem. Phys.* **2011**, *13*, 15891–15898.

(45) Korshin, D. E.; Kashapov, R. R.; Murtazina, L. I.; Mukhitova, R. K.; Kharlamov, S. V; Latypov, S. K.; Ryzhkina, I. S.; Ziganshina, A. Y.; Konovalov, A. I. Self-Assembly of an Aminoalkylated Resorcinarene in Aqueous Media: Host–Guest Properties. *New J. Chem.* **2009**, *33*, 2397–2401.

(46) Bucur, C. B.; Sui, Z.; Schlenoff, J. B. Ideal Mixing in Polyelectrolyte Complexes and Multilayers: Entropy Driven Assembly. *J. Am. Chem. Soc.* **2006**, *128*, 13690–13691.

(47) Mansikkamäki, H.; Nissinen, M.; Rissanen, K. Noncovalent Π···π-Stacked Exo-Functional Nanotubes: Subtle Control of Resorcinarene Self-Assembly. *Angew. Chem. Int. Ed.* **2004**, *43*, 1243–1246.

(48) Beyeh, N. K.; Göth, M.; Kaufmann, L.; Schalley, C. A.; Rissanen, K. The Synergetic Interplay of Weak Interactions in the Ion-Pair Recognition of Quaternary and Diquaternary Ammonium Salts by Halogenated Resorcinarenes. *Eur. J. Org. Chem.* **2014**, 80–85.

(49) Mansikkamäki, H.; Schalley, C. A.; Nissinen, M.; Rissanen, K. Weak Interactions between Resorcinarenes and Diquaternary Alkyl Ammonium Cations. *New J. Chem.* **2005**, *29*, 116–127.

(50) Mansikkamäki, H.; Nissinen, M.; Rissanen, K. C-Methyl Resorcin[4]Arene Packing Motifs with Alkyl Ammonium Salts: From Molecular Capsules to Channels and Tubes. *CrystEngComm* **2005**, *7*, 519–526.

(51) Beyeh, N. K.; Weimann, D. P.; Kaufmann, L.; Schalley, C. A.; Rissanen, K. Ion-Pair Recognition of Tetramethylammonium Salts by Halogenated Resorcinarenes. *Chem. – A Eur. J.* **2012**, *18*, 5552–5557.

(52) Han, X.; Tian, C.; Gandra, I.; Eslava, V.; Galindres, D.; Vargas, E.; Leblanc, R. The Investigation on Resorcinarenes towards either Inhibiting or Promoting Insulin Fibrillation. *Chem. – A Eur. J.* **2017**, *23*, 17903–17907.

(53) Jang, Y-M.; Yu, C-J.; Kim, J-S.; Kim, S-U. Ab initio design of drug carriers for zoledronate guest molecule using phosphonated and sulfonated calix[4]arene and calix[4]resorcinarene host molecules. *J. Mater. Sci.* **2018**, *53*, 5125–5139.

(54) Mercer, S. M.; Robert, T.; Dixon, D. V; Chen, C.-S.; Ghoshouni, Z.; Harjani, J. R.; Jahangiri, S.; Peslherbe, G. H.; Jessop, P. G. Design, Synthesis and Solution Behaviour of Small Polyamines as Switchable Water Additives. *Green Chem.* **2012**, *14*, 832–839.

(55) Rigaku Oxford Diffraction, **2017**, *CrysAlisPro* software system, version 38.46, Rigaku Corporation, Oxford, UK.

(56) Sheldrick, G. M. A Short History of SHELX. *Acta Crystallogr.* **2008**, *A64*, 112–122.

(57) Sheldrick, G. M. Crystal Structure Refinement with SHELXL. *Acta Crystallogr.* **2015**, *C71*, 3–8.

(58) Dolomanov, O. V; Bourhis, L. J.; Gildea, R. J.; Howard, J. A. K.; Puschmann, H. OLEX2: A Complete Structure Solution, Refinement and Analysis Program. *J. Appl. Crystallogr.* **2009**, *42*, 339–341.

(59) Frisch, M. J.; Trucks, G. W.; Schlegel, H. B.; Scuseria, G. E.; Robb, M. A.; Cheeseman, J. R.; Scalmani, G.; Barone, V.; Petersson, G. A.; Nakatsuji, H.; Li, X.; Caricato, M.; Marenich, A. V.; Bloino, J.; Janesko, B. G.; Gomperts, R.; Mennucci, B.; Hratchian, H. P.; Ortiz, J. V.; Izmaylov, A. F.; Sonnenberg, J. L.; Williams-Young, D.; Ding, F.; Lipparini, F.; Egidi, F.; Goings, J.; Peng, B.; Petrone, A.; Henderson, T.; Ranasinghe, D.; Zakrzewski, V. G.; Gao, J.; Rega, N.; Zheng, G.; Liang, W.; Hada, M.; Ehara, M.; Toyota, K.; Fukuda, R.; Hasegawa, J.; Ishida, M.; Nakajima, T.; Honda, Y.; Kitao, O.; Nakai, H.; Vreven, T.; Throssell, K.; Montgomery, J. A., Jr.; Peralta, J. E.; Ogliaro, F.; Bearpark, M. J.; Heyd, J. J.; Brothers, E. N.; Kudin, K. N.; Staroverov, V. N.; Keith, T. A.; Kobayashi, R.; Normand, J.; Raghavachari, K.; Rendell, A. P.; Burant, J. C.; Iyengar, S. S.; Tomasi, J.; Cossi, M.; Millam, J. M.; Klene, M.; Adamo, C.; Cammi, R.; Ochterski, J. W.; Martin, R. L.; Morokuma, K.; Farkas, O.; Foresman, J. B.; Fox, D. J. Gaussian 16, Revision C.01, Gaussian, Inc., Wallingford CT, **2016**

(60) Perdew, J. P.; Ernzerhof, M.; Burke, K. Rationale for Mixing Exact Exchange with Density Functional Approximations. *J. Chem. Phys.* **1996**, *105*, 9982–9985.

(61) Perdew, J. P.; Burke, K.; Ernzerhof, M. Generalized Gradient Approximation Made Simple. *Phys. Rev. Lett.* **1996**, *77*, 3865–3868.

(62) Perdew, J. P.; Burke, K.; Ernzerhof, M. Generalized Gradient Approximation Made Simple. [Phys. Rev. Lett. 77, 3865 (1996)]. *Phys. Rev. Lett.* **1997**, *78*, 1396.

(63) Adamo, C.; Barone, V. Toward Reliable Density Functional Methods without Adjustable Parameters: The PBE0 Model. *J. Chem. Phys.* **1999**, *110*, 6158–6170.

(64) Schäfer, A.; Huber, C.; Ahlrichs, R. Fully Optimized Contracted Gaussian Basis Sets of Triple Zeta Valence Quality for Atoms Li to Kr. *J. Chem. Phys.* **1994**, *100*, 5829–5835.

(65) Grimme, S.; Ehrlich, S.; Goerigk, L. Effect of the Damping Function in Dispersion

Corrected Density Functional Theory. *J. Comput. Chem.* **2011**, *32*, 1456–1465.

"For Table of Contents Use Only"

Host-Guest Interactions of Sodiumsulfonatomethyleneresorcinarene and Quaternary Ammonium Halides: An Experimental-Computational Analysis of the Guest Inclusion Properties

Kwaku Twum,[a] J. Mikko Rautiainen,[b] Shilin Y. Yu,[b] Khai-Nghi K. N. Truong,[b] Jordan Feder,[a] Kari Rissanen,[b] Rakesh Puttreddy[b,c*] and Ngong Kodiah Beyeh[a*]

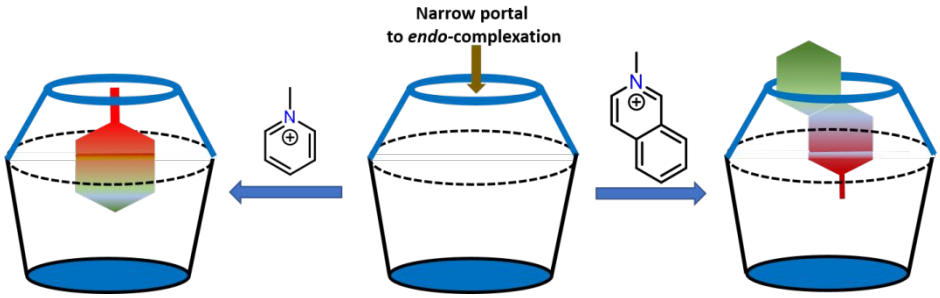

A combination of ^{1}H NMR spectroscopy, isothermal titration calorimetry, X-ray crystallography and computational studies were used to investigate the host-guest chemistry of a two-component system, sodiumsulfonatomethyleneresorcinarene (**An**) and ammonium guests (**Bn**), in hydrogen bond competing solvent (MeOH-d_4).